Cyanine Masking: A Strategy to Test Functional Group Effects on Antibody Conjugate Targeting

Ek Raj Thapaliya,[1] Syed Muhammad Usama,[1] Nimit L. Patel,[2] Yang Feng,[3] Joseph D. Kalen,[2] Brad St. Croix,[3] Martin J. Schnermann[1*]

[1]Chemical Biology Laboratory, Center for Cancer Research, National Cancer Institute, Frederick, Maryland 21702, United States

[2]Small Animal Imaging Program, Frederick National Laboratory for Cancer Research, Leidos Biomedical Research Inc., Frederick, Maryland 21702, United States

[3]Tumor Angiogenesis Unit, Mouse Cancer Genetics Program (MCGP), National Cancer Institute, NIH, Frederick, Maryland 21702, United States

Email: martin.schnermann@nih.gov

ABSTRACT

Conjugates of small molecule and antibodies are broadly employed diagnostic and therapeutic agents. Appending a small molecule to an antibody often significantly impacts the properties of the resulting conjugate. Here we detail a systematic study investigating the effect of various functional groups on the properties of antibody-fluorophore conjugates. This was done through the preparation and analysis of a series of masked heptamethine cyanines (CyMasks) bearing amides with varied functional groups. These were designed to exhibit a broad range of physical properties, and include hydrophobic (-NMe_2), pegylated (NH-PEG-8 or NH-PEG-24), cationic (NH-$(CH_2)_2NMe_3^+$) anionic (NH-$(CH_2)_2SO_3^-$), and zwitterionic (N-$(CH_2)_2NMe_3^+$)-$(CH_2)_3SO_3^-$) variants. The CyMask series was appended to tumor targeting monoclonal antibodies (mAbs) and analyzed for effects on tumor targeting, clearance and non-specific organ uptake. Among the series, zwitterionic and cationic dye conjugates showed the highest tumor-to-background ratio (TBR), although the latter also exhibited an elevated liver-to-background ratio (LBR). Overall, these studies provide a strategy to test the functional group effects and suggest that zwitterionic substituents are an attractive strategy to mask hydrophobic payloads, with the potential to improve the properties of bioconjugates *in vivo*.

KEYWORDS. antibody fluorophore conjugates, in vivo optical imaging, drug delivery, fluorescence guided surgery, tumor imaging

TOC GRAPHIC

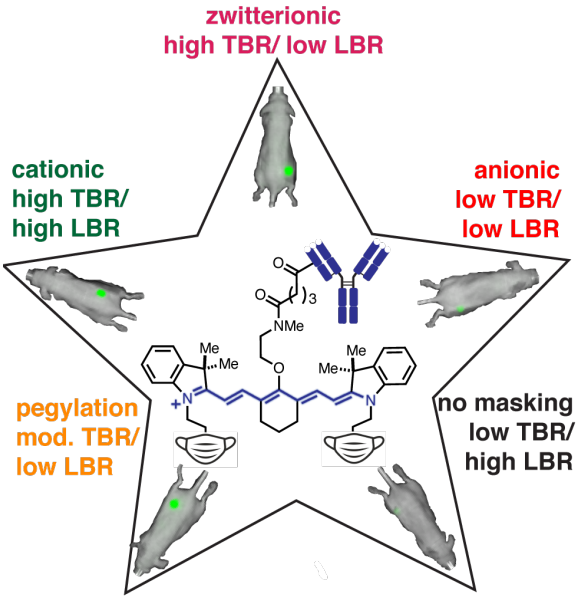

INTRODUCTION

Conjugates of monoclonal antibodies (mAbs) and small molecules are indispensable tools for diagnostic and therapeutic applications. While long used for various cellular imaging applications (i.e. immunolabeling), the last decade has seen significant progress in the translation of mAb conjugates into clinical settings. For example, conjugates of fluorescent molecules and mAbs have emerged as powerful tumor imaging agents for fluorescence guided surgery.[1, 2] In the context of therapeutics, antibody drug conjugates (ADCs) harness the specificity of antibodies to selectively deliver potent payload molecules.[3] Despite significant progress validating these approaches, significant challenges remain. In particular, many small molecule payloads interfere with the intrinsic targeting and clearance of the parent antibody.[4-6] Various strategies are being explored to circumvent this issue. These include homogenous labeling strategies, which have been explored extensively for ADCs. While such strategies improve certain *in vivo* properties, they increase the complexity of the labeling process.[7-9] For optical probes, the use of highly charged, persulfonated fluorophores is a long established strategy designed to address the issue of fluorophore aggregation on the protein surface.[10] This strategy led to the creation of numerous broadly-used fluorophores, including the "Cy" and "Alexa Fluor" series. While these probes are optimized for *in vitro* efforts, more recent results from our group and others have shown that the highly charged, but net neutral (i.e. zwitterionic) fluorophores can improve the targeting of mAbs *in vitro* and *in vivo*.[16]

A critical, still outstanding question is what functional group can best mitigate the impact of small molecule labeling on mAb targeting? Here, we pursue a strategy centered on comparing the antibody conjugates of a series of modified near-infrared (NIR) fluorescent dyes. While intrinsically hydrophobic, these molecules can be synthetically modified with polar functional groups. Several prior studies, including from our group, have examined the impact of modifications on the *in vivo* properties of mAb-fluorophore conjugates.[11-16,17,18,19-21] While these prior studies provided key insights, they are not systematic from a "functional-group" perspective making it hard to draw larger lessons (See Figure S1 for previously tested molecules). Here we address this issue with single point alterations to substituents distal to the cyanine scaffold. We hypothesize that this approach will provide insights that can broadly inform the design of various bioconjugates.

Below we detail the synthesis and evaluation of a series of masked heptamethine cyanines (CyMasks) and their antibody conjugates. These probes enable the unbiased assessment of chemical masking strategies on tumor targeting and off-target accumulation of mAb conjugates. In line with prior results, we find that the most hydrophobic probe exhibits the most non-selective *in vitro* uptake and the lowest *in vivo* tumor targeting. We also find that anionic and cationic masking groups lead to increased dye aggregation and reduced tumor signal. Notably, pegylated probes, which have been broadly applied in other contexts,[22-27] exhibit excellent *in vitro* uptake, but reduce *in vivo* tumor targeting. By contrast, zwitterionic probes, bearing both quaternary ammonium and sulfonate functional groups, exhibit excellent *in vitro* and *in vivo* properties. We hypothesize that the combination of highly charged, but net neutral, substituents may offer significantly improved biophysical properties with implications to a range of bioconjugates.

RESULTS AND DISCUSSION

Synthesis and Characterization of CyMask and mAb Conjugates

In designing the CyMask series, we sought to examine a range of polar substituents and chose representative zwitterionic, cationic, anionic, pegylated and hydrophobic functional groups. Specifically, we synthesized six CyMask dyes containing amides substituted with PEG-8, PEG-24, *N*-ethyl-sulfonate (Sulfo), *N*-ethyl-trimethyl-ammonium (Quat), *N*-trimethyl-propyl-ammonium-*N*-butyl-sulfonate (Zwit) and, a hydrophobic derivative, methylamine (Me). As shown in Scheme 1, the CyMask-NHS esters were synthesized from the known precursor (**1**) using our previously reported Smiles rearrangement method.[11] Compound **1** underwent substitution with *N*-methyl-ethanolamine in MeCN at 80 °C to obtain **2**. The subsequent Smiles rearrangement (C4′-*N* to C4′-*O* alkylation) reaction was carried out using an initial TFA induced rearrangement, followed by electrophilic trapping in THF in the presence of $NaHCO_3$ at 50 °C to give methyl ester **3**. This common precursor **3** was used to couple with primary amines **4a-f** to give amides **5a-f** and subsequent saponification with LiOH provided the free carboxylic acids (**6a-f**). We compared the

photophysical properties of all six CyMask carboxylic acids (**6a-f**) and found similar optical properties in PBS pH 7.4 and 10% FBS (Table 1, Figure S2,S3) across this series and relative to other C4′-*O*-linked heptamethine cyanines.[11-16] These observations confirm the minimal impact of the distal modification on the optical properties of the free molecules.

Scheme 1: Synthesis of compounds in CyMask series and conjugation with Panitumumab.

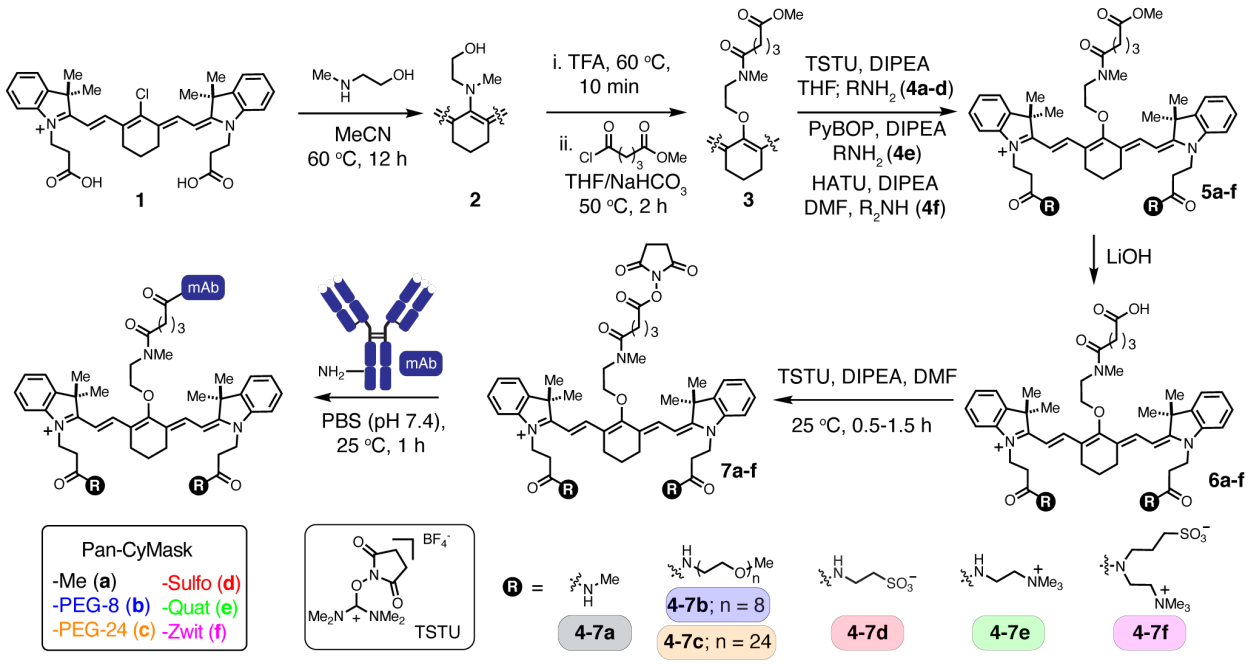

Table 1: Key Spectroscopic Properties.

CyMask-CO_2H	$\lambda_{max,abs}$ (nm)	$\lambda_{max,em}$ (nm)	Φ_F	ε^a (M^{-1} cm^{-1})	brightness ($\varepsilon \times \Phi_F$)	net surface charge
CyMask-Me-CO_2H (**6a**)	766	781	0.14	161000	22,500	0
CyMask-PEG-8-CO_2H (**6b**)	766	781	0.13	203000	26,400	0
CyMask-PEG-24-COOH (**6c**)	766	781	0.15	182300	27,500	0
CyMask-Sulfo-CO_2H(**6d**)	764	780	0.11	174000	19,000	-2
CyMask-Quat-CO_2H (**6e**)	764	780	0.12	184000	22,000	+2
CyMask-Zwit-CO_2H(**6f**)	764	780	0.11	184000	20,240	0

a. Molar absorption coefficient of all dyes was measured in 1:1 MeOH-PBS pH 7.4.

We then sought to examine the impact of the masking functional group on the properties of mAb conjugates. The carboxylic acids **6a-f** (CyMask-CO_2H) were converted to CyMask-NHS esters (**7a-f**) using *N*,*N*,*N*′,*N*′-tetramethyl-O-(N-succinimidyl) uronium tetrafluoroborate (TSTU) and used in the bioconjugation step. We choose to first generate conjugates with Panitumumab (Pan), an anti-EGFR FDA-approved monoclonal antibody, which has been used extensively by us and others for imaging applications.[11-16] All six NHS esters were reacted with panitumumab (Pan) in 50 mM PBS pH 7.4 with molar excesses of 3, 6 and 10X to obtain the lysine labeled Pan conjugates with a degree of labeling (DOL) of 1, 2, 3 (±0.3), respectively. Two purification methods were applied to remove unlabeled probe. The dye conjugates were passed through a spin desalting column and stored overnight at 4 °C to dissociate non-covalently bound free dyes. The resulting solutions were purified a second time by passing through a desalting column eluting with PBS pH 7.4. All conjugates provided homogenous solutions with stable absorption spectra over a several month timeframe.

The photophysical properties of these mAb-CyMask conjugates were analyzed in detail. The absorbance spectra were recorded in PBS pH 7.4 (Figure 1). While displaying nearly identical absorbance maxima, significant variation in the H-aggregate peak at 700 nm (Figure 1a insert) was observed across the various conjugates in PBS, but not in denaturing conditions (1:1 PBS:MeOH, Figure S5). This peak, which results from cyanine dimerization on the protein surface, is a well characterized consequence of protein labeling.[28-30] The magnitude of the H-aggregate was found to be dependent on both the probe and the DOL.[31-33] As a convenient means to quantify these effects, we examined the ratio of the absorbance values 766 (monomer) and 700 (dimer) nm (Figure 1a-d). Across the series, the values decrease along series Sulfo > Me > Zwit > PEG-8 > Quat > PEG-24. Notably, PEG-24 provided almost complete inhibition of H-aggregate formation, as noted elsewhere.[23, 34] The observation that sulfonated substituents led to the most substantial H-aggregate formation is somewhat surprising. Prior results clearly indicate that sulfonates appended to the indolenine heterocycles improve the properties of the resulting mAb conjugates.[29, 30, 35, 36] However, these results suggest that distal sulfonates are not sufficient to inhibit H-aggregation, and may even induce formation. Lastly, we evaluated the quantum yield (Φ_F) of the mAb conjugates at DOL 3. Notably, Φ_F of thee conjugates did not vary dramatically (4.8% to 7.5%) in PBS pH 7.2 (Figure 1e). Additionally, we observe little correlation between Φ_F with either H-aggregation or the *in vivo* results described below. These observations suggest that the photon output of the fluorophore-mAb conjugates is relatively insensitive to the CyMask functional group, which simplifies the analysis of the *in vivo* data reported below.

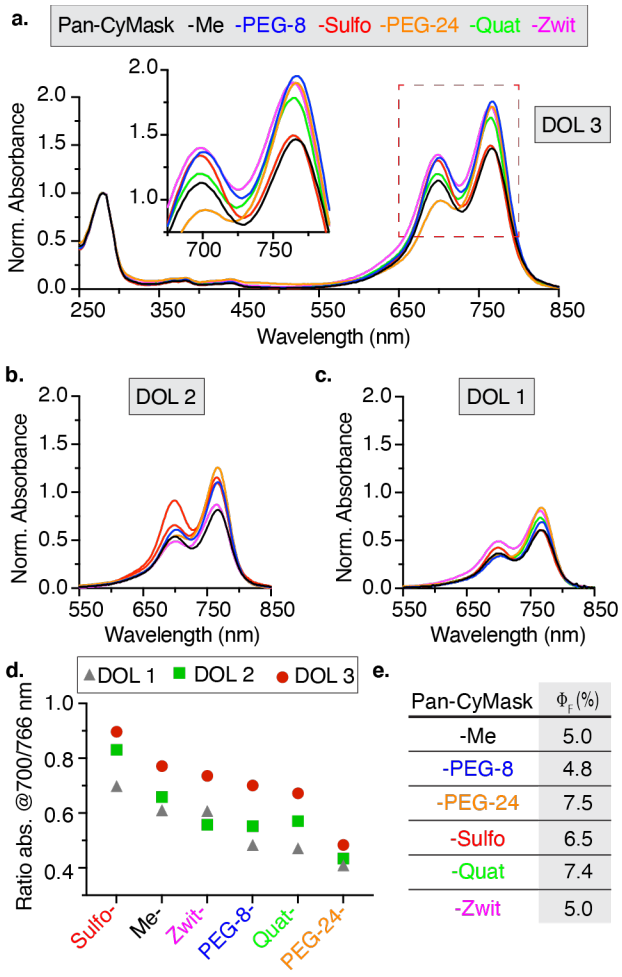

Figure 1. Characterization of Pan-CyMask conjugates. **a.** Normalized absorption of Pan-CyMask conjugates (DOL 3, PBS pH 7.2). Zoomed in spectra is depicted in inset. **b**. Normalized absorption of Pan-CyMask conjugates (DOL 2, PBS pH 7.2). c. Normalized absorption spectra of Pan-CyMask (DOL 1, PBS pH 7.2). **d.** Aggregation ratio (absorbance ratio at 700/766 nm) of Pan-CyMask conjugates at DOL 1, 2 and 3, calculated from absorption spectra. **e.** Φ_F (measured by relative method) Pan-CyMask conjugates (DOL 3, PBS pH 7.2).

Comparison of Panitumumab-CyMask Conjugates

We sought to characterize the impact of the CyMask modifications on tumor targeting and biodistribution of these agents. These studies were carried out using athymic nude female mice bearing EGFR+ MDA-MB-468 xenografts implanted subcutaneously in the right flank (5×10^6 cells, n = 5 per group).[16] The mice were injected with 50 μg of the Pan-CyMask conjugates (DOL 3). Fluorescence images were obtained using an IVIS imaging system before injection and at 4, 24, 48, 72 and 168 h post injection. As early as 4h, all the conjugates showed significant tumor signal, which increased over the next 7 days (Figure 2a, S6-7). After 7 days, the highest radiance fluorescence intensity was observed with the Zwit- and Quat- conjugates, with values that are ~5.5 and 5.0-fold higher compared to Me- conjugate, respectively. Analysis of the

tumor-to-background ratio (TBR) indicates a rank order Zwit ≈ Quat > PEG-24 > Sulfo ≈ PEG-8 ≈ Me 1-week p.i. (Figure 2b-c). While the fluorescence signal in most healthy organs remain low, significant background uptake was observed in liver, specifically for cationic and anionic dye conjugates, with strongest signal at the 4 h time point (Figure 2d, S6-7). Of note, the *in vivo* imaging data was confirmed in subsequent *ex vivo* study using Pan-CyMask-Zwit and Pan-CyMask-Me conjugates, where mice (n = 3 per group) were analyzed *ex vivo* at 48 h p.i. (Figure S8). *Ex vivo* histopathological analysis of tumor slices injected with Pan-CyMask-Zwit and Pan-CyMask-Me showed heterogenous near infrared signal throughout the tumor with highest signal around vasculature (Figure 2e, S9). In the tissue samples, we observed ~2X higher fluorescent labeling in tumors with Pan-CyMask-Zwit (~20-30%) as compared to Pan-CyMask-Me (~10-20%). Overall, these results indicate the zwitterionic conjugates outperform the charged conjugates (Sulfo and Quat) with respective to liver uptake. Additionally, the zwitterionic conjugates improved mAb tumor uptake relative to hydrophobic, anionic and pegylated conjugates.

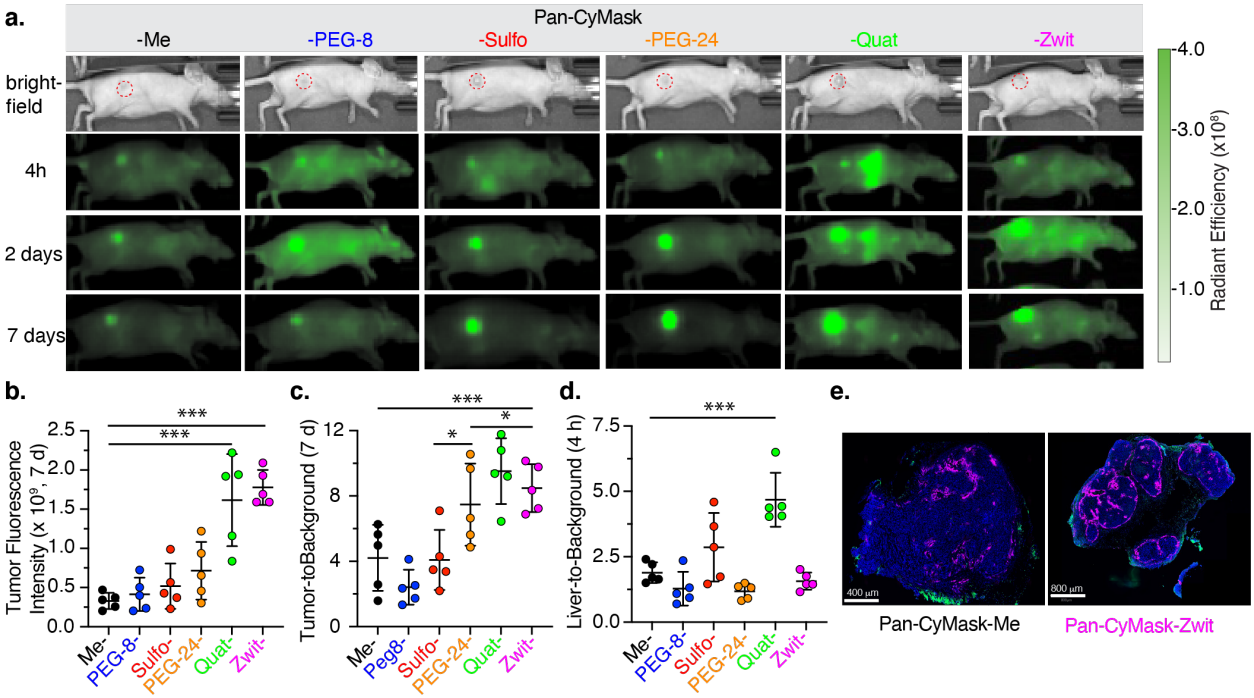

Figure 2. *In vivo* and ex-vivo fluorescence imaging of MDA- MB-468 xenograft tumor bearing mice injected with 50 µg of each Pan-CyMask conjugates at DOL 3. **a.** *In vivo* fluorescence images (right dorsum) at pre-injection, and 4 h, 2 days and 7 days post-injection (p.i.). **b.** Tumor signal (total radiant efficiency normalized to tumor size), **c.** tumor to background ratio, **d.** liver to background ratio of MDA-MB-468 tumor-bearing mice injected with 50 µg of six Pan-CyMask conjugates at DOL 3. Statistical analysis was performed between groups at 7 days using Student's t-test. * p-value ≤ 0.05, *** p-value ≤ 0.001. **e.** Representative histopathological images of tumor tissue sections (48 h, post injection) with Pan-CyMask-Me and Pan-CyMask-Zwit. The image is pseudo colored: pink (near infrared channel;Cy7), blue (DAPI) and green (autofluorescence).

We then studied the cellular uptake of these fluorophore conjugates in EGFR+ (MDA-MB-468) or EGFR- (MCF-7) cell lines. Epifluorescence microscopy demonstrated the high specific uptake of these dye conjugates in MDA-MB-468 cells compared to the control cells line MCF-7, when incubated with the same concentration of Pan-CyMask conjugates and incubation time (250 μg/mL, 7h) (Figure 3a). This approach indicates similar cellular uptake of all six Pan-CyMask conjugates. We quantified these differences in more detail by determining an apparent binding constant (EC_{50}) using flow cytometry for three of the conjugates. The Pan-CyMask-PEG-24 conjugate showed slightly lower binding affinity (EC_{50} =7.6 nM) compared to the Pan-CyMask-Zwit- (EC_{50} = 4.5 nM) or Pan-CyMask-Me (EC_{50} =6.9 nM) (Figure 3b). Overall, these data studies suggest modest differences in *in vitro* cellular uptake between the CyMask series, and suggest that *in vivo* differences are largely due to altered clearance.

Next we investigated a potential for hepatic clearance pathway using an *in vitro* cellular model. Prior work examining the uptake of ADCs and other conjugates has revealed a critical role for stellate macrophages, or Kupffer cells, in mediating the uptake and clearance of bioconjugates labeled with hydrophobic payloads.[37, 38] To study the effect of the masking group on dye conjugates with respect to the non-specific uptake, we examined the uptake of these dye conjugates in rat Kupffer cells using flow cytometry.[38] After incubation of Pan-CyMask conjugates with rat Kupffer cells for 24 h, the most hydrophobic dye conjugate, Pan-CyMask-Me, exhibited increased uptake compared to other conjugates (Figure 3c). Notably, irrespective of the nature of the masking group, more hydrophilic dye conjugates showed similar non-specific uptake by Kupffer cells. These results are in line with the prior observations suggesting a role for Kupffer cells in the uptake of hydrophobic small molecule-mAb conjugates, but suggest that additional mechanisms maybe be at play for the high uptake of the positively charged Pan-CyMask-Quat conjugate *in vivo.*

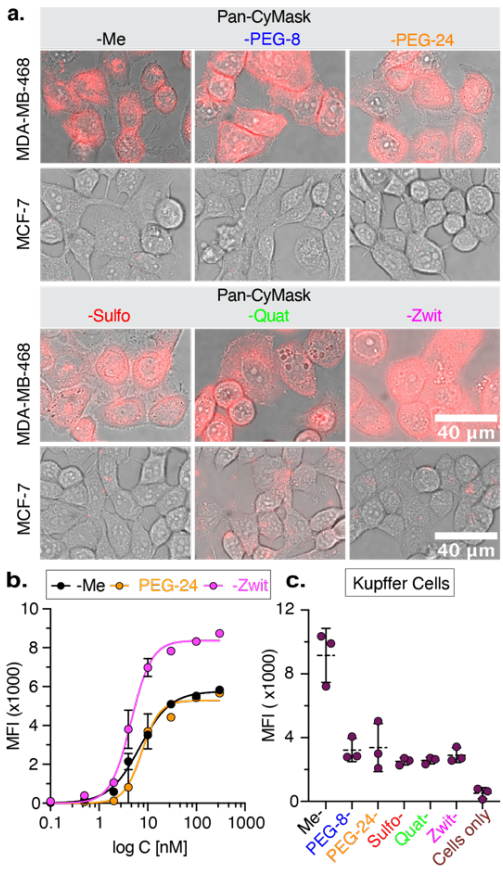

Figure 3. *In vitro* studies of Pan-CyMask conjugates in MDA-MB-468 (EGFR+), MCF-7 (EGFR-) and Kupffer cells. **a.** Epifluorescence imaging of cells after 7 h incubation of Pan-CyMask conjugates (250 µg/mL) for MDA-MB-468 (top row) and MCF-7 (bottom row). **b**. Binding affinity of Pan-CyMask conjugates in MDA-MB-468 cells. Cells were incubated with CyMask-Pan conjugates (0.1-0.3 µM) at ice bath for 1h in PBS pH 7.4 with 1 mg/mL of BSA containing 0.01% sodium azide and fixed. Mean Fluorescence Intensity (MFI ± SD, n = 3) was measured by flow cytometry. **c**. Non-specific uptake of mAb conjugates in Kupffer cells. Cells were incubated with Pan-CyMask conjugates 0.1 mg/mL at 37° C for 24 h in serum-containing media, MFI ± SD (n = 3) was measured by flow cytometry.

Comparison of anti-CD-276 mAb-CyMask Conjugates

To test the generality of these observations, we applied CyMask with a fully-human anti-CD276 (B7 homolog H3, B7H3) antibody that binds both mouse CD276 and human CD276 with similar affinity.[39, 40] This target is overexpressed in the cancer cells and tumor neovasculature of multiple solid tumor types, and this antibody has been applied to create potent ADCs.[39-44] For the *in vivo* studies we chose to compare the effects of positive charge (Quat), no charge (Me) and net neutral charge (Zwit) CyMask on tumor targeting and clearance. The conjugates were injected intravenously into mice bearing 200-250 mm^3 JIMT-1 breast tumors grown orthotopically in the mammary fat pad. The tumor fluorescence intensity and TBR was highest for the m276-SL-CyMask-Zwit (10.2) after 7 days (Figure 4a-b, S10-11). These studies provide additional evidence that zwitterionic masking can improve the properties of mAb conjugates.

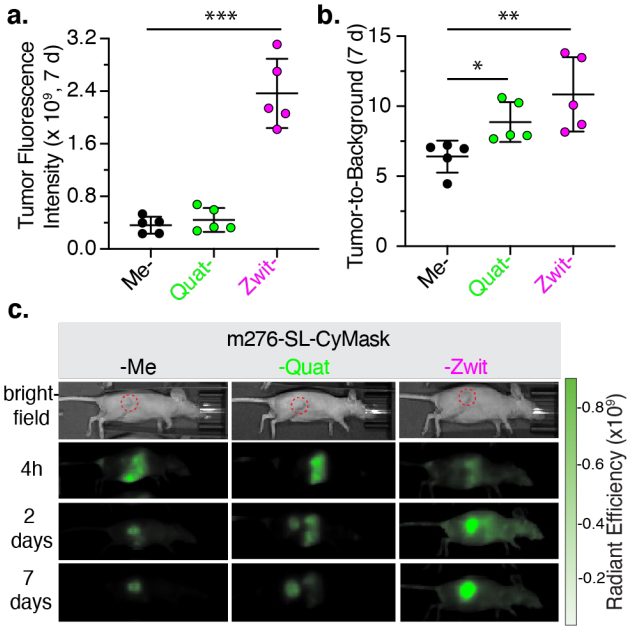

Figure 4. **a.** Quantification of tumor uptake of m276-SL-CyMask-Me, Quat and Zwit conjugates (50 μg; DOL 3) in JIMT-1 tumors after 168 h. **b.** Tumor-to-Background ratio at 168 h post injection. **C.** IVIS images at 4 h, 2 days and 7 days post injection. Tumor are highlighted in red dotted circles. Statistical analysis was performed between groups at 168h. Data points are displayed as mean ± SD, and the p-values were evaluated by the Student's t-test (* p-value ≤ 0.05, ** p-value ≤ 0.01, *** p-value ≤ 0.001).

Conclusion

In the studies outlined above, we detail an unbiased comparison of charge masking functional groups on the *in vivo* targeting properties of mAb-fluorophore conjugates. These studies reveal that zwitterionic and cationic shielding outperform pegylated, anionic, and hydrophobic conjugates with respect to tumor uptake. Furthermore, cationic shielding leads to the highest off-target liver uptake at early imaging time points. Notably, significant *in vitro* non-specific uptake by Kupffer cells occurs with the hydrophobic derivative, but not the charged or pegylated conjugates. In total, these results suggest the zwitterionic shielding groups may offer the optimal combination of excellent targeting and minimal off-target uptake. These results that align with prior studies from our group and others, which found zwitterionic heptamethine cyanines exhibit improved tumor uptake when compared to conventional persulfonated heptamethine cyanines.[16,17,45]

These observations complement prior work to optimize the *in vivo* properties of therapeutic protein and nano-material modalities. In particular, extensive efforts have investigated the impact of mAb sequence modifications on clearance and tumor targeting. The general theme to emerge from these efforts is that cationization and anionization – the introduction of positively and negatively charged amino acids, respectively - both increase plasma clearance rate, albeit through different mechanisms.[46] Cationization

generally increases tissue uptake, which can be advantageous for solid tumor uptake, but also leads to increased uptake in off-target organs.[47] By contrast, anionization decreases tissue uptake due to increased whole-body (including blood) clearance through enhanced hepatic clearance.[46] In general, these studies have settled on the notion that the isoelectric point (i.e. the pH at which the protein is net neutral) of native antibodies, which is typically between 7-8, is preferred. While efforts to chemically introduce charged functional groups, as we have done here, are rare, extensive efforts have examined the impact of pegylation strategies.[23, 34, 47-51] While offering significant benefits with respect to plasma half-life, this approach increases the size of protein significantly with consequent impacts on binding interactions.[52-55] Additionally, particularly when appended to long half-life proteins, such as mAbs, there is a potential for antibody mediated immune responses.[56-58]

Complementing efforts to augment the properties of proteins, the nanomaterials community has extensively studied the impact of charge and polarity as passivation strategies to improve the properties of otherwise hydrophobic species. In this context, there is significant evidence that zwitterionic functional groups reduce nonspecific adsorption at the particle/liquid interface.[37, 59] The resulting decrease in non-specific interactions leads to reduced off-target uptake in various contexts. While, the exact mechanism of this effect isn't entirely clear, previous studies have suggested a combination of charge shielding, minimization of membrane penetration, and protein stabilization.[60]

Here we introduce a series of optical probes that enable the quantitative assessment of functional group effects on mAb-targeting *in vivo*. These results suggest that zwitterionic functional groups – which are highly charged, but net neutral modifications - may represent an important addition to the mAb-bioconjugate landscape. This strategy, which maintains the original charge profile of the parent protein, and simultaneously introduces a highly charged functional group, may represent a promising approach to mask the undesirable hydrophobicity of drug-conjugates in the circulation. Future studies will investigate the potential impact of these modification in homogeneous mAb conjugates, where we hypothesize that charge will also play a significant role.[61, 62] Additionally, we suggest that the incorporation of such zwitterionic functional groups into otherwise hydrophobic therapeutic payloads may have significant promise. Studies toward this goal are underway in our group, and will be reported in due course.

ASSOCIATED CONTENT

Supporting Information

This material is available free of charge via the internet at http://pubs.acs.org. The supporting information contains synthesis procedures, characterization of CyMask probes, key intermediate compounds, photophysical properties of CyMask probes, details of in vitro and in vivo experiments and supporting figures and tables.

AUTHOR INFORMATION

* *Email: martin.schnermann@nih.gov*

ACKNOWLEDGMENTS

This work was supported by the Intramural Research Program of the National Institutes of Health (NIH), NCI-CCR. It was also supported by an NCI CCR FLEX Program Synergy Award (to M.S. and B.S.C.) and a Congressionally Directed Medical Research Program (CDRMP) Breast Cancer Research Program grant (award number W81WXH21-1-0109). We acknowledge Dr. James A. Kelley (National Cancer Institute) for providing the high-resolution mass spectrometry analysis. We thank Dr. Gary T. Pauly (National Cancer Institute) for assisting with LC/MS and HPLC purification. The Biophysics Resource, CCR is acknowledged for use of instrumentation. We would also like to thank Dr. Jeff Carrell (CCR-Frederick Flow Cytometry Core Laboratory) for assisting with flow cytometry and Dr. Elijah F. Edmondson (Molecule Histopathology Laboratory, Leidos Biomedical Research) for *ex vivo* analyzing histopathology samples.

REFERENCES

1. Joshi, B. P.; Wang, T. D., Targeted Optical Imaging Agents in Cancer: Focus on Clinical Applications. *Contrast Media Mol Imaging* **2018,** *2018*, 2015237.
2. Rosenthal, E. L.; Warram, J. M.; de Boer, E.; Chung, T. K.; Korb, M. L.; Brandwein-Gensler, M.; Strong, T. V.; Schmalbach, C. E.; Morlandt, A. B.; Agarwal, G.; Hartman, Y. E.; Carroll, W. R.; Richman, J. S.; Clemons, L. K.; Nabell, L. M.; Zinn, K. R., Safety and Tumor Specificity of Cetuximab-IRDye800 for Surgical Navigation in Head and Neck Cancer. *Clin Cancer Res* **2015,** *21* (16), 3658-66.
3. Chari, R. V.; Miller, M. L.; Widdison, W. C., Antibody-drug conjugates: an emerging concept in cancer therapy. *Angewandte Chemie* **2014,** *53* (15), 3796-827.
4. Usama, S. M.; Thapaliya, E. R.; Luciano, M. P.; Schnermann, M. J., Not so innocent: Impact of fluorophore chemistry on the in vivo properties of bioconjugates. *Curr Opin Chem Biol* **2021,** *63*, 38-45.
5. Donaghy, H., Effects of antibody, drug and linker on the preclinical and clinical toxicities of antibody-drug conjugates. *Mabs-Austin* **2016,** *8* (4), 659-71.
6. Buecheler, J. W.; Winzer, M.; Weber, C.; Gieseler, H., Alteration of Physicochemical Properties for Antibody-Drug Conjugates and Their Impact on Stability. *J Pharm Sci* **2020,** *109* (1), 161-168.
7. Agarwal, P.; Bertozzi, C. R., Site-specific antibody-drug conjugates: the nexus of bioorthogonal chemistry, protein engineering, and drug development. *Bioconjug Chem* **2015,** *26* (2), 176-92.
8. Panowski, S.; Bhakta, S.; Raab, H.; Polakis, P.; Junutula, J. R., Site-specific antibody drug conjugates for cancer therapy. *Mabs-Austin* **2014,** *6* (1), 34-45.
9. Sochaj, A. M.; Swiderska, K. W.; Otlewski, J., Current methods for the synthesis of homogeneous antibody-drug conjugates. *Biotechnol Adv* **2015,** *33* (6), 775-784.
10. Ernst, L. A.; Gupta, R. K.; Mujumdar, R. B.; Waggoner, A. S., Cyanine dye labeling reagents for sulfhydryl groups. *Cytometry* **1989,** *10* (1), 3-10.
11. Nani, R. R.; Shaum, J. B.; Gorka, A. P.; Schnermann, M. J., Electrophile-Integrating Smiles Rearrangement Provides Previously Inaccessible C4′-O-Alkyl Heptamethine Cyanine Fluorophores. *Organic Letters* **2015,** *17* (2), 302-305.
12. Sato, K.; Nagaya, T.; Nakamura, Y.; Harada, T.; Nani, R. R.; Shaum, J. B.; Gorka, A. P.; Kim, I.; Paik, C. H.; Choyke, P. L.; Schnermann, M. J.; Kobayashi, H., Impact of C4′-O-Alkyl Linker on in

Vivo Pharmacokinetics of Near-Infrared Cyanine/Monoclonal Antibody Conjugates. *Molecular Pharmaceutics* **2015,** *12* (9), 3303-3311.
13. Sato, K.; Gorka, A. P.; Nagaya, T.; Michie, M. S.; Nakamura, Y.; Nani, R. R.; Coble, V. L.; Vasalatiy, O. V.; Swenson, R. E.; Choyke, P. L.; Schnermann, M. J.; Kobayashi, H., Effect of charge localization on the: In vivo optical imaging properties of near-infrared cyanine dye/monoclonal antibody conjugates. *Molecular BioSystems* **2016,** *12* (10), 3046-3056.
14. Sato, K.; Gorka, A. P.; Nagaya, T.; Michie, M. S.; Nani, R. R.; Nakamura, Y.; Coble, V. L.; Vasalatiy, O. V.; Swenson, R. E.; Choyke, P. L.; Schnermann, M. J.; Kobayashi, H., Role of Fluorophore Charge on the in Vivo Optical Imaging Properties of Near-Infrared Cyanine Dye/Monoclonal Antibody Conjugates. *Bioconjugate Chemistry* **2016,** *27* (2), 404-413.
15. Cha, J.; Nani, R. R.; Luciano, M. P.; Kline, G.; Broch, A.; Kim, K.; Namgoong, J. M.; Kulkarni, R. A.; Meier, J. L.; Kim, P.; Schnermann, M. J., A chemically stable fluorescent marker of the ureter. *Bioorganic and Medicinal Chemistry Letters* **2018,** *28* (16), 2741-2745.
16. Luciano, M. P.; Crooke, S. N.; Nourian, S.; Dingle, I.; Nani, R. R.; Kline, G.; Patel, N. L.; Robinson, C. M.; Difilippantonio, S.; Kalen, J. D.; Finn, M. G.; Schnermann, M. J., A Nonaggregating Heptamethine Cyanine for Building Brighter Labeled Biomolecules. *ACS Chemical Biology* **2019,** *14* (5), 934-940.
17. Li, D.-H.; Schreiber, C. L.; Smith, B. D., Sterically Shielded Heptamethine Cyanine Dyes for Bioconjugation and High Performance Near-Infrared Fluorescence Imaging. *Angewandte Chemie International Edition* **2020,** *59* (29), 12154-12161.
18. Yazaki, P.; Lwin, T.; Minnix, M.; Li, L.; Sherman, A.; Molnar, J.; Miller, A.; Frankel, P.; Chea, J.; Poku, E.; Bowles, N.; Hoffman, R.; Shively, J.; Bouvet, M., Improved antibody-guided surgery with a near-infrared dye on a PEGylated linker for CEA-positive tumors. *Journal of Biomedical Optics* **2019,** *24* (6), 066012.
19. Rodell, C. B.; Baldwin, P.; Fernandez, B.; Weissleder, R.; Sridhar, S.; Dubach, J. M., Quantification of Cellular Drug Biodistribution Addresses Challenges in Evaluating in vitro and in vivo Encapsulated Drug Delivery. *Adv Ther (Weinh)* **2021,** *4* (3).
20. Thurber, G. M.; Yang, K. S.; Reiner, T.; Kohler, R. H.; Sorger, P.; Mitchison, T.; Weissleder, R., Single-cell and subcellular pharmacokinetic imaging allows insight into drug action in vivo. *Nat Commun* **2013,** *4*, 1504.
21. Cilliers, C.; Menezes, B.; Nessler, I.; Linderman, J.; Thurber, G. M., Improved Tumor Penetration and Single-Cell Targeting of Antibody-Drug Conjugates Increases Anticancer Efficacy and Host Survival. *Cancer Res* **2018,** *78* (3), 758-768.
22. Simmons, J. K.; Burke, P. J.; Cochran, J. H.; Pittman, P. G.; Lyon, R. P., Reducing the antigen-independent toxicity of antibody-drug conjugates by minimizing their non-specific clearance through PEGylation. *Toxicol Appl Pharmacol* **2020,** *392*, 114932.
23. Lyon, R. P.; Bovee, T. D.; Doronina, S. O.; Burke, P. J.; Hunter, J. H.; Neff-LaFord, H. D.; Jonas, M.; Anderson, M. E.; Setter, J. R.; Senter, P. D., Reducing hydrophobicity of homogeneous antibody-drug conjugates improves pharmacokinetics and therapeutic index. *Nat Biotechnol* **2015,** *33* (7), 733-5.
24. Zhao, R. Y.; Wilhelm, S. D.; Audette, C.; Jones, G.; Leece, B. A.; Lazar, A. C.; Goldmacher, V. S.; Singh, R.; Kovtun, Y.; Widdison, W. C.; Lambert, J. M.; Chari, R. V., Synthesis and evaluation of hydrophilic linkers for antibody-maytansinoid conjugates. *J Med Chem* **2011,** *54* (10), 3606-23.
25. Moon, S. J.; Govindan, S. V.; Cardillo, T. M.; D'Souza, C. A.; Hansen, H. J.; Goldenberg, D. M., Antibody conjugates of 7-ethyl-10-hydroxycamptothecin (SN-38) for targeted cancer chemotherapy. *J Med Chem* **2008,** *51* (21), 6916-26.
26. Miller, M. L.; Roller, E. E.; Zhao, R. Y.; Leece, B. A.; Ab, O.; Baloglu, E.; Goldmacher, V. S.; Chari, R. V., Synthesis of taxoids with improved cytotoxicity and solubility for use in tumor-specific delivery. *J Med Chem* **2004,** *47* (20), 4802-5.
27. King, H. D.; Dubowchik, G. M.; Mastalerz, H.; Willner, D.; Hofstead, S. J.; Firestone, R. A.; Lasch, S. J.; Trail, P. A., Monoclonal antibody conjugates of doxorubicin prepared with branched peptide

linkers: inhibition of aggregation by methoxytriethyleneglycol chains. *J Med Chem* **2002,** *45* (19), 4336-43.
28. Gruber, H. J.; Hahn, C. D.; Kada, G.; Riener, C. K.; Harms, G. S.; Ahrer, W.; Dax, T. G.; Knaus, H. G., Anomalous fluorescence enhancement of Cy3 and cy3.5 versus anomalous fluorescence loss of Cy5 and Cy7 upon covalent linking to IgG and noncovalent binding to avidin. *Bioconjug Chem* **2000,** *11* (5), 696-704.
29. Pauli, J.; Grabolle, M.; Brehm, R.; Spieles, M.; Hamann, F. M.; Wenzel, M.; Hilger, I.; Resch-Genger, U., Suitable labels for molecular imaging--influence of dye structure and hydrophilicity on the spectroscopic properties of IgG conjugates. *Bioconjug Chem* **2011,** *22* (7), 1298-308.
30. Pauli, J.; Pochstein, M.; Haase, A.; Napp, J.; Luch, A.; Resch-Genger, U., Influence of Label and Charge Density on the Association of the Therapeutic Monoclonal Antibodies Trastuzumab and Cetuximab Conjugated to Anionic Fluorophores. *Chembiochem* **2017,** *18* (1), 101-110.
31. Rijpkema, M.; Bos, D. L.; Cornelissen, A. S.; Franssen, G. M.; Goldenberg, D. M.; Oyen, W. J.; Boerman, O. C., Optimization of Dual-Labeled Antibodies for Targeted Intraoperative Imaging of Tumors. *Mol Imaging* **2015,** *14*, 348-55.
32. Cohen, R.; Stammes, M. A.; de Roos, I. H.; Stigter-van Walsum, M.; Visser, G. W.; van Dongen, G. A., Inert coupling of IRDye800CW to monoclonal antibodies for clinical optical imaging of tumor targets. *EJNMMI Res* **2011,** *1* (1), 31.
33. Conner, K. P.; Rock, B. M.; Kwon, G. K.; Balthasar, J. P.; Abuqayyas, L.; Wienkers, L. C.; Rock, D. A., Evaluation of near infrared fluorescent labeling of monoclonal antibodies as a tool for tissue distribution. *Drug Metab Dispos* **2014,** *42* (11), 1906-13.
34. Burke, P. J.; Hamilton, J. Z.; Jeffrey, S. C.; Hunter, J. H.; Doronina, S. O.; Okeley, N. M.; Miyamoto, J. B.; Anderson, M. E.; Stone, I. J.; Ulrich, M. L.; Simmons, J. K.; McKinney, E. E.; Senter, P. D.; Lyon, R. P., Optimization of a PEGylated Glucuronide-Monomethylauristatin E Linker for Antibody-Drug Conjugates. *Mol Cancer Ther* **2017,** *16* (1), 116-123.
35. Mujumdar, R. B.; Ernst, L. A.; Mujumdar, S. R.; Lewis, C. J.; Waggoner, A. S., Cyanine Dye Labeling Reagents - Sulfoindocyanine Succinimidyl Esters. *Bioconjugate Chemistry* **1993,** *4* (2), 105-111.
36. Mujumdar, S. R.; Mujumdar, R. B.; Grant, C. M.; Waggoner, A. S., Cyanine-labeling reagents: Sulfobenzindocyanine succinimidyl esters. *Bioconjugate Chem* **1996,** *7* (3), 356-362.
37. Longmire, M.; Choyke, P. L.; Kobayashi, H., Clearance properties of nano-sized particles and molecules as imaging agents: considerations and caveats. *Nanomedicine (Lond)* **2008,** *3* (5), 703-17.
38. Meyer, D. W.; Bou, L. B.; Shum, S.; Jonas, M.; Anderson, M. E.; Hamilton, J. Z.; Hunter, J. H.; Wo, S. W.; Wong, A. O.; Okeley, N. M.; Lyon, R. P., An in Vitro Assay Using Cultured Kupffer Cells Can Predict the Impact of Drug Conjugation on in Vivo Antibody Pharmacokinetics. *Mol Pharm* **2020,** *17* (3), 802-809.
39. Seaman, S.; Zhu, Z.; Saha, S.; Zhang, X. M.; Yang, M. Y.; Hilton, M. B.; Morris, K.; Szot, C.; Morris, H.; Swing, D. A.; Tessarollo, L.; Smith, S. W.; Degrado, S.; Borkin, D.; Jain, N.; Scheiermann, J.; Feng, Y.; Wang, Y.; Li, J.; Welsch, D.; DeCrescenzo, G.; Chaudhary, A.; Zudaire, E.; Klarmann, K. D.; Keller, J. R.; Dimitrov, D. S.; St Croix, B., Eradication of Tumors through Simultaneous Ablation of CD276/B7-H3-Positive Tumor Cells and Tumor Vasculature. *Cancer Cell* **2017,** *31* (4), 501-515 e8.
40. Kendsersky, N. M.; Lindsay, J.; Kolb, E. A.; Smith, M. A.; Teicher, B. A.; Erickson, S. W.; Earley, E. J.; Mosse, Y. P.; Martinez, D.; Pogoriler, J.; Krytska, K.; Patel, K.; Groff, D.; Tsang, M.; Ghilu, S.; Wang, Y.; Seaman, S.; Feng, Y.; Croix, B. S.; Gorlick, R.; Kurmasheva, R.; Houghton, P. J.; Maris, J. M., The B7-H3-Targeting Antibody-Drug Conjugate m276-SL-PBD Is Potently Effective Against Pediatric Cancer Preclinical Solid Tumor Models. *Clin Cancer Res* **2021,** *27* (10), 2938-2946.
41. Qin, X.; Zhang, H.; Ye, D.; Dai, B.; Zhu, Y.; Shi, G., B7-H3 is a new cancer-specific endothelial marker in clear cell renal cell carcinoma. *Onco Targets Ther* **2013,** *6*, 1667-73.
42. Zang, X.; Sullivan, P. S.; Soslow, R. A.; Waitz, R.; Reuter, V. E.; Wilton, A.; Thaler, H. T.; Arul, M.; Slovin, S. F.; Wei, J.; Spriggs, D. R.; Dupont, J.; Allison, J. P., Tumor associated endothelial expression of B7-H3 predicts survival in ovarian carcinomas. *Mod Pathol* **2010,** *23* (8), 1104-12.

43. Brunner, A.; Hinterholzer, S.; Riss, P.; Heinze, G.; Brustmann, H., Immunoexpression of B7-H3 in endometrial cancer: relation to tumor T-cell infiltration and prognosis. *Gynecol Oncol* **2012,** *124* (1), 105-11.
44. Seaman, S.; Stevens, J.; Yang, M. Y.; Logsdon, D.; Graff-Cherry, C.; St Croix, B., Genes that distinguish physiological and pathological angiogenesis. *Cancer Cell* **2007,** *11* (6), 539-54.
45. Choi, H. S.; Nasr, K.; Alyabyev, S.; Feith, D.; Lee, J. H.; Kim, S. H.; Ashitate, Y.; Hyun, H.; Patonay, G.; Strekowski, L.; Henary, M.; Frangioni, J. V., Synthesis and In Vivo Fate of Zwitterionic Near-Infrared Fluorophores. *Angew Chem Int Edit* **2011,** *50* (28), 6258-6263.
46. Boswell, C. A.; Tesar, D. B.; Mukhyala, K.; Theil, F. P.; Fielder, P. J.; Khawli, L. A., Effects of charge on antibody tissue distribution and pharmacokinetics. *Bioconjug Chem* **2010,** *21* (12), 2153-63.
47. Lee, H. J.; Pardridge, W. M., Monoclonal antibody radiopharmaceuticals: cationization, pegylation, radiometal chelation, pharmacokinetics, and tumor imaging. *Bioconjug Chem* **2003,** *14* (3), 546-53.
48. Lee, W.; Bobba, K. N.; Kim, J. Y.; Park, H.; Bhise, A.; Kim, W.; Lee, K.; Rajkumar, S.; Nam, B.; Lee, K. C.; Lee, S. H.; Ko, S.; Lee, H. J.; Jung, S. T.; Yoo, J., A short PEG linker alters the in vivo pharmacokinetics of trastuzumab to yield high-contrast immuno-PET images. *J Mater Chem B* **2021,** *9* (13), 2993-2997.
49. Guillou, A.; Earley, D. F.; Klingler, S.; Nisli, E.; Nuesch, L. J.; Fay, R.; Holland, J. P., The Influence of a Polyethylene Glycol Linker on the Metabolism and Pharmacokinetics of a (89)Zr-Radiolabeled Antibody. *Bioconjug Chem* **2021,** *32* (7), 1263-1275.
50. Sano, K.; Nakajima, T.; Miyazaki, K.; Ohuchi, Y.; Ikegami, T.; Choyke, P. L.; Kobayashi, H., Short PEG-linkers improve the performance of targeted, activatable monoclonal antibody-indocyanine green optical imaging probes. *Bioconjug Chem* **2013,** *24* (5), 811-6.
51. Chapman, A. P., PEGylated antibodies and antibody fragments for improved therapy: a review. *Adv Drug Deliv Rev* **2002,** *54* (4), 531-45.
52. Gokarn, Y. R.; McLean, M.; Laue, T. M., Effect of PEGylation on protein hydrodynamics. *Mol Pharm* **2012,** *9* (4), 762-73.
53. Takashina, K.; Kitamura, K.; Yamaguchi, T.; Noguchi, A.; Noguchi, A.; Tsurumi, H.; Takahashi, T., Comparative pharmacokinetic properties of murine monoclonal antibody A7 modified with neocarzinostatin, dextran and polyethylene glycol. *Jpn J Cancer Res* **1991,** *82* (10), 1145-50.
54. Kitamura, K.; Takahashi, T.; Yamaguchi, T.; Noguchi, A.; Noguchi, A.; Takashina, K.; Tsurumi, H.; Inagake, M.; Toyokuni, T.; Hakomori, S., Chemical engineering of the monoclonal antibody A7 by polyethylene glycol for targeting cancer chemotherapy. *Cancer Res* **1991,** *51* (16), 4310-5.
55. Suzuki, T.; Kanbara, N.; Tomono, T.; Hayashi, N.; Shinohara, I., Physicochemical and biological properties of poly(ethylene glycol)-coupled immunoglobulin G. *Biochim Biophys Acta* **1984,** *788* (2), 248-55.
56. Elsadek, N. E.; Hondo, E.; Shimizu, T.; Takata, H.; Abu Lila, A. S.; Emam, S. E.; Ando, H.; Ishima, Y.; Ishida, T., Impact of Pre-Existing or Induced Anti-PEG IgM on the Pharmacokinetics of Peginterferon Alfa-2a (Pegasys) in Mice. *Mol Pharm* **2020,** *17* (8), 2964-2970.
57. Yang, Q.; Lai, S. K., Anti-PEG immunity: emergence, characteristics, and unaddressed questions. *Wiley Interdiscip Rev Nanomed Nanobiotechnol* **2015,** *7* (5), 655-77.
58. Justin T. Huckaby, T. M. J., Zhongbo Li, Robert J. Perna, Anting Wang, Nathan I. Nicely & Samuel K. Lai, Structure of an anti-PEG antibody reveals an open ring that captures highly flexible PEG polymers. *Communications Chemistry* **2020**.
59. Schlenoff, J. B., Zwitteration: coating surfaces with zwitterionic functionality to reduce nonspecific adsorption. *Langmuir* **2014,** *30* (32), 9625-36.
60. Erfani, A.; Seaberg, J.; Aichele, C. P.; Ramsey, J. D., Interactions between Biomolecules and Zwitterionic Moieties: A Review. *Biomacromolecules* **2020,** *21* (7), 2557-2573.
61. Debie, P.; Van Quathem, J.; Hansen, I.; Bala, G.; Massa, S.; Devoogdt, N.; Xavier, C.; Hernot, S., Effect of Dye and Conjugation Chemistry on the Biodistribution Profile of Near-Infrared-Labeled Nanobodies as Tracers for Image-Guided Surgery. *Molecular Pharmaceutics* **2017,** *14* (4), 1145-1153.

62. Luciano, M. P.; Dingle, I.; Nourian, S.; Schnermann, M. J., Preferential Light-Chain Labeling of Native Monoclonal Antibodies Improves the Properties of Fluorophore Conjugates. *Tetrahedron Lett* **2021,** *75*.